Droplet Breakup and Shear-Induced Mixing in Critical Polymer Blends†

Sanghoon Kim, Erik K. Hobbie,* Jae-Woong Yu, and Charles C. Han

Polymers Division, National Institute of Standards and Technology, Gaithersburg, Maryland 20899

Received May 30, 1997; Revised Manuscript Received September 26, 1997⊗

ABSTRACT: Phase-contrast microscopy, small-angle light scattering, and fluorescence microscopy have been combined *in situ* to study domain deformation, breakup, and homogenization in unstable mixtures of polystyrene (PS) and polybutadiene (PB) under shear flow. Close to the critical point, mixing of the two components toward a single homogeneous phase occurs via repeated deformation and fragmentation of minority-phase droplets, and the data are in good agreement with the mode-coupling renormalization-group (MCRG) theory of a simple binary mixture under shear flow. Well into the two-phase region of diluted high-molecular-weight PS/PB blends, however, the data suggest a tendency for $T_c(\dot{\gamma})$ to saturate at very high shear rates.

I. Introduction

The morphology of polymer blends under shear is of great practical importance in polymer processing and engineering. Because of the small entropy of mixing associated with long-chain macromolecules, most homopolymer mixtures are immiscible.[1] In a typical application, two components are "homogenized" in the presence of a flow field. The actual flows encountered in polymer processing are nontrivial functions of geometry, flow rate, temperature, composition, and molecular weight. An expansion of the velocity field $\mathbf{v}(\mathbf{r})$ around a given position, however, frequently reduces the local flow condition to one of simple shear, or $v_x(y) \approx \dot{\gamma}y$, where the quantity $\dot{\gamma} = \partial v_x/\partial y$ is defined as the shear rate. The physics of two-phase polymer flows in a constant velocity gradient is thus of fundamental interest.

There is a remarkable degree of complexity surrounding polymeric fluids under shear, and a universal description is clearly a challenging task. The aim of many blending techniques,[2] however, is to control the domain morphology, often via the introduction of reactive components or compatibilizers. For blends in the vicinity of a critical point of unmixing, a useful starting point is the mode-coupling renormalization-group (MCRG) theory of a simple binary fluid under shear.[3−5] The advantage of such an approach is that it incorporates static and dynamic "critical-fluctuation" effects associated with segregation in binary fluids that have been demonstrated to be important in polymer blends over a surprisingly wide range of temperatures and molecular weights.[6−10]

Although the shear response of small-molecule mixtures is consistent with the MCRG theory,[11] the slow relaxation times characteristic of macromolecular systems permit a unique and rigorous test. Small-angle neutron scattering (SANS) has been a powerful tool for such studies, and agreement with theory is quite good in the miscible or "one-phase" region of the phase diagram, where structures on the order of several chain dimensions are easily sheared apart by the flow.[12,13] From a practical perspective, however, the response of the blend in the unstable or "two-phase" regime is of greater interest. The *in situ* combination of light scattering and digital-video microscopy (Figure 1) is an extremely powerful tool for studying the morphology of polymer blends under shear.[14−18] Close to the critical point, the response of the mixture can be explained by combining classical hydrodynamics[19−21] with the MCRG theory. Well into the equilibrium two-phase region of high-molecular-weight systems, however, such a description appears to break down in a way that may have implications for the flow-induced blending of macromolecules.

II. Background

A. Shear Suppression of Critical Fluctuations in the One-Phase Region. The MCRG theory of a simple binary fluid has been used by a number of authors to model the critical dynamics and shear response of macromolecular mixtures and solutions.[22−25] In the quiescent or equilibrium limit $\dot{\gamma} = 0$, it reduces to model H in the Hohenberg−Halperin classification scheme.[26] The effect of the shear appears in the equation of motion for the order parameter $\psi(\mathbf{r},t) = \phi(\mathbf{r},t) - \phi_0$, which represents local deviations from the uniform composition ϕ_0. The essential physics of the mode-coupling argument lies in the hydrodynamic coupling between ψ and the velocity field. Long-wavelength composition fluctuations are transported and deformed by the viscous motion of the fluid, and the flow stabilizes an anisotropic steady state away from thermodynamic equilibrium. In polymer blends, critical fluctuations lead to a crossover from mean-field to Ising behavior, and the window around T_c where mean-field theory breaks down can be quite large.[6−10] The subtle interplay between mode-coupling and Ising-critical effects is the foundation of the MCRG description,[27] which predicts a suppression of the critical temperature by the shear as represented schematically in Figure 2. That flow would have a mixing effect on a two component fluid is intuitive, although the details of the theory itself are quite complicated.

The response of the mixture depends on how large $\dot{\gamma}$ is compared to $1/\tau_c$, where τ_c is the order-parameter relaxation time. In low-molecular-weight mixtures, τ_c can be measured with SANS and dynamic light scat-

† Errors bars used in graphs and figures denote best estimates of two standard deviations in the total experimental uncertainty. According to ISO 31-8, the term "molecular weight" has been replaced by "relative molar mass". The conventional notation, rather than the ISO notation, has been used in this publication.

⊗ Abstract published in *Advance ACS Abstracts,* December 1, 1997.

S0024-9297(97)00764-X

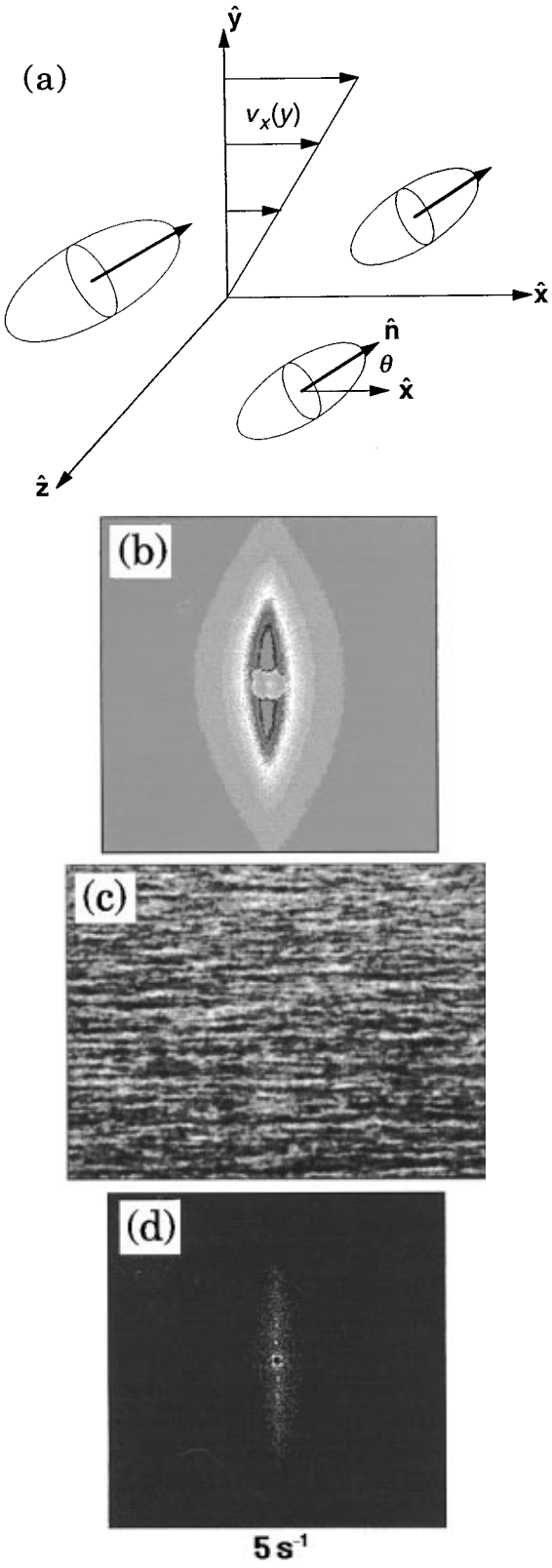

Figure 1. (a) Velocity gradient in the $\hat{\mathbf{y}}$ direction elongating droplets at an angle θ with respect to the flow ($\hat{\mathbf{x}}$) direction, while rotating them around the vorticity ($\hat{\mathbf{z}}$) axis. The angle θ decreases from $\pi/4$ with increasing shear. *In-situ* light-scattering patterns (b), phase-contrast micrographs (c), and numerically calculated structure factors (d) give information about droplet deformation and breakup. In b−d, the $\hat{\mathbf{x}}$ direction is from left to right, the $\hat{\mathbf{z}}$ direction is from bottom to top, and the $\hat{\mathbf{y}}$ direction is into the page. The micrograph width throughout this paper is 200 μm, and the width of the light-scattering pattern always corresponds to a scattering angle of 52° (±27°). The fluid is a 60/40 blend of polystyrene/polybutadiene ($3 \times 10^3/3 \times 10^3$) at 132.2 °C.

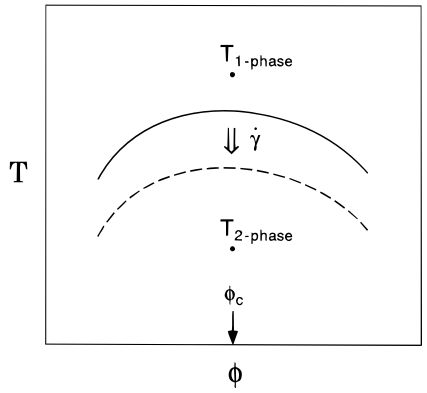

Figure 2. Schematic representation of shear-induced mixing in a binary fluid. For temperatures in the one-phase region where long-wavelength fluctuations are stable, the critical point moves away with increasing shear rate. For temperatures in the two-phase region where these fluctuations become unstable and grow into domains, the critical point moves closer with increasing shear rate.

tering,[12,28] making it convenient to define a reduced, dimensionless shear rate $\tilde{\gamma} = \tau_c\dot{\gamma}$ that resembles a Deborah number in appearance. For a binary fluid that exhibits critical fluctuations, SANS gives a correlation length and susceptibility, $\xi(\dot{\gamma})$ and $S(\dot{\gamma})$, respectively, that reflect the shear-induced shift in T_c.[29] Reducing these quantities by their equilibrium values and plotting them as a function of $\tilde{\gamma}$ give a universal scaling curve containing no free parameters. This has been demonstrated in both low-molecular-weight[12] and diluted high-molecular-weight[13] blends and reveals the intuitive result that composition fluctuations are suppressed when $\tilde{\gamma} \geq 1$, or $\dot{\gamma} \geq 1/\tau_c$. The relaxation time, correlation length, and susceptibility all become quite large at the critical point, where long-wavelength structures are easily sheared apart by the flow.

B. Two-Phase Hydrodynamics near a Critical Point. Most studies of two-phase hydrodynamics cite the classic work by Taylor on isolated droplets in definable fields of flow.[19−21] The Taylor model is a steady-state solution of the incompressible Navier−Stokes equation at low Reynolds number ($Re = \rho R^2\dot{\gamma}/\eta$, where ρ is the density, R is the droplet radius, and η is the viscosity) assuming an initially spherical droplet. For the viscosities and droplet sizes of interest, $Re < 1$ over the range of $\dot{\gamma}$ considered here. The mixtures are either sufficiently close to a critical point or sufficiently dilute in a common good solvent such that the viscosities of the two phases do not differ radically. When this is the case, a spherical droplet is deformed into an ellipsoid of major axis $R_{||}$ and minor axis $R_\perp$ (Figure 1a), with the aspect ratio

$$\zeta = R_{||}/R_\perp \approx (1 + x)/(1 - x) + \ldots \qquad (1)$$

where $x = \tau\dot{\gamma}$. The quantity $\tau = \eta R/\sigma$ is the droplet stress−relaxation time, where σ is the interfacial tension. A droplet breaks into fragments when the shear stress becomes comparable to the capillary pressure or when $\dot{\gamma}$ reaches a threshold value $\dot{\gamma}_c \sim \sigma/2\eta R$. At low $\dot{\gamma}$, the axis of elongation of the ellipsoid (Figure 1a) points along the principal rate-of-strain direction ($\theta = \pi/4$), but as the domains elongate, θ decreases to $\sim \pi/9$ in the vicinity of the breakup. Since $\dot{\gamma}_c$ depends on R, larger droplets break at lower shear rates. Monodisperse distributions on the order of the breakup size have been observed in far-from-critical mixtures under shear.[30]

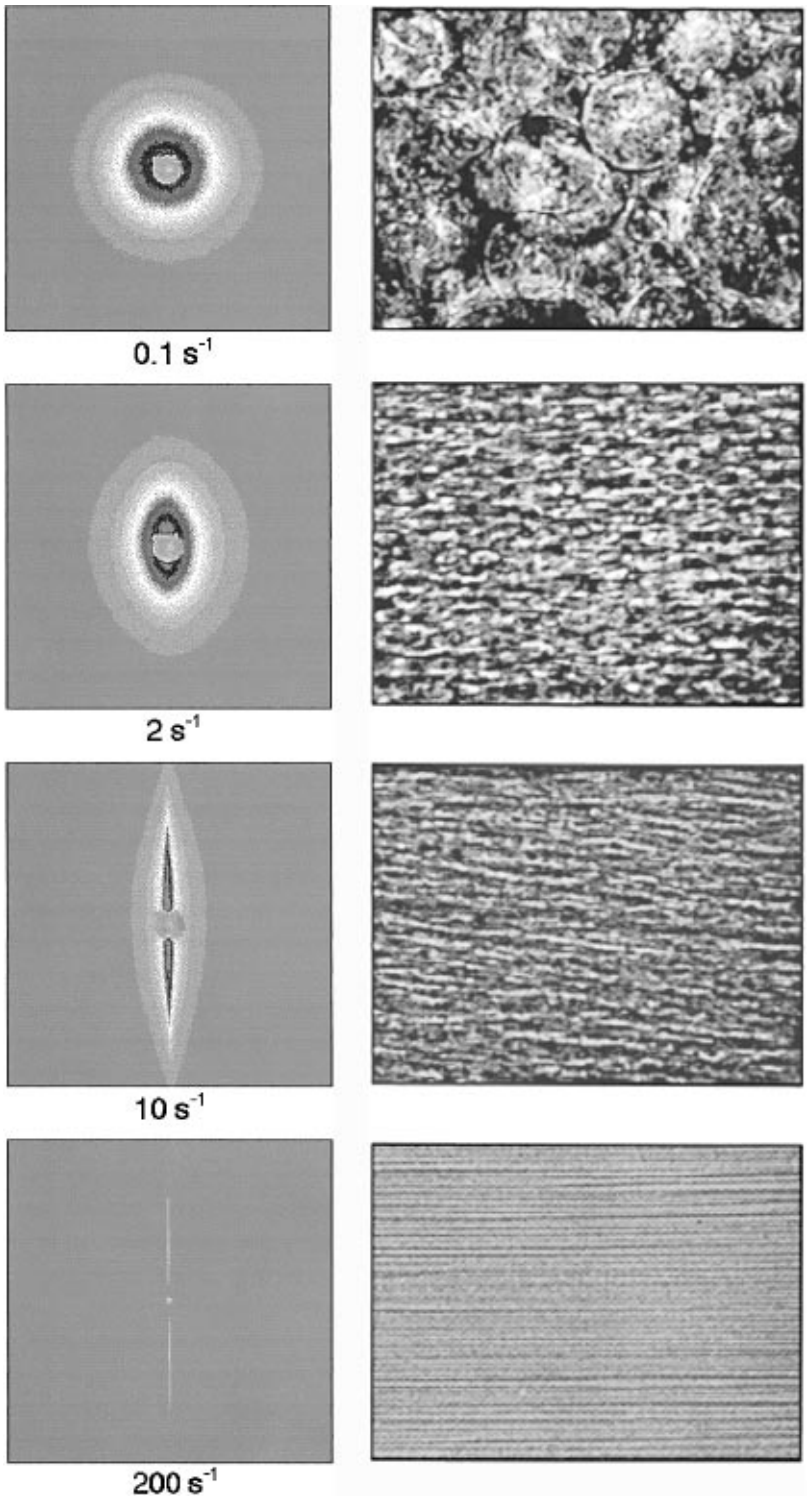

Figure 3. Light-scattering/micrograph pair as a function of shear rate for a coexisting low-molecular-weight [60/40 PS/PB ($3 \times 10^3/3 \times 10^3$)] critical blend. The geometry is as specified in Figure 1. The temperature of 132.7 °C is 1.5 K below the equilibrium T_c. Stabilized in the weak-shear limit, droplets of the minority phase first elongate and then fragment repeatedly, eventually giving way to a stringlike morphology in the strong shear limit. The extreme anisotropy of the domains becomes inverted in q space.

An extension of the Taylor model to a thermodynamically unstable binary fluid has been made by Onuki.[4,5] In the weak-shear limit,[31] the mixture reaches a steady state in which the thermodynamic instability is "stabilized" by the flow. As $\dot{\gamma}$ increases, droplets of the minority phase elongate and break repeatedly as in the Taylor model.[32] Close to criticality in the strong-shear limit,[31] the domains become highly elongated along the direction of flow, giving way to a stringlike morphology with a structure factor that exhibits extreme anisotropy. In the MCRG description, this behavior is intimately linked to critical fluctuations. The surface tension in a critical fluid is $\sigma \sim 0.1 k_B T/\xi^2$.[33] The shear-induced shift in T_c leads to a softening of σ via an *increase* in ξ as the mixture is effectively pushed closer to the phase boundary by the flow (Figure 2). To leading order in $\epsilon = 4 - d$ (d is the spatial dimension), the MCRG theory[3] gives

$$\sigma(\dot{\gamma}) = \sigma_0\{1 - A(\tau_{c0}\dot{\gamma})^{1/3\nu}\}^{2\nu} \qquad (2)$$

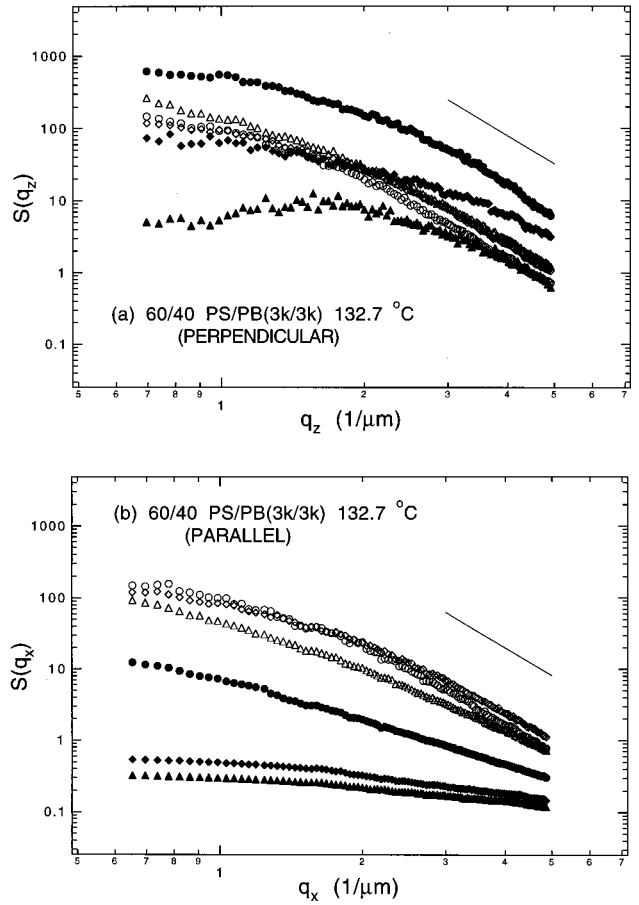

Figure 4. Log−log plots of the projection of the scattering intensity (a) normal and (b) along the flow direction for the data shown in Figure 3. The shear rates are 0.1 (open circles), 0.5 (open diamonds), 2 (open triangles), 10 (filled circles), 50 (filled diamonds), and 200 s^{-1} (filled triangles). The lines represent asymptotic Porod (q^{-4}) behavior.

where σ_0 is the surface tension in the $\dot{\gamma} \rightarrow 0$ limit, A is a universal amplitude of $O(\epsilon)$, ν is the critical exponent associated with ξ, and $\tau_{c0} = \eta\langle R\rangle/\sigma_0$ is the average weak-shear ("bare") stress−relaxation time. Each time a droplet ruptures, the composition difference between droplet and matrix decreases, which lowers the droplet surface tension. As a consequence, individual droplets can sustain higher and higher deformation before breaking.[32]

III. Experiment

A. Materials and Measurements. The mixtures used in this study were pure blends of low-molecular-weight ($3 \times 10^3/3 \times 10^3$) polystyrene (PS) and polybutadiene (PB) and moderate-to-high-molecular-weight ($96.4 \times 10^3/22 \times 10^3$) PS/PB blends in a common good solvent of dioctylphthalate (DOP). For fluorescence-microscopy measurements, the PS has been labeled with the fluorescent dye 4-chloro-7-nitrobenzofurazan (NBD chloride), which slightly modifies the molecular weight to 110×10^3. The molecular-weight distributions were reasonably monodisperse with polydispersity indices M_w/M_n ranging from around 1.02 to 1.10. All of the diluted blends were prepared at 8% total weight fraction polymer in DOP. Optical turbidity measurements were used to map out the coexistence curve as a function of composition and temperature. The critical composition (temperature) in the pure low-molecular-weight blends is around 60/40 PS/PB (134.2 °C), while that in the diluted high-molecular-weight blends is 30/70 PS/PB (68.0 °C) for the unlabeled PS, and 30/70 PS(F)/PB (86.5 °C) for the labeled PS. For all of the mixtures considered here, critical fluctuations lead to a crossover from mean-field to Ising behavior in the vicinity of T_c.

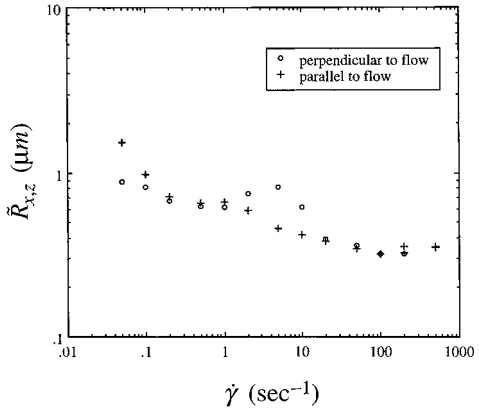

Figure 5. Length-scales $\tilde{R}_x(\dot{\gamma})$ and $\tilde{R}_z(\dot{\gamma})$ obtained from fitting $S(q_x)$ and $S(q_z)$ to eq 3 for the light-scattering data shown in Figures 3 and 4. A similar decrease with shear rate is observed in the diluted high-molecular-weight PS/PB blends, although with a slightly larger dynamic range perpendicular to the flow direction.

Phase-contrast-microscopy, small-angle-light-scattering, and fluorescence-microscopy measurements were all carried out *in situ* on phase-separating polymer blends under shear flow using the instrument described elsewhere.[15] The optical contrast between the two phases is reasonably small ($n_{PS} = 1.59$, $n_{PB} = 1.51$, and $n_{DOP} = 1.49$) such that multiple-scattering effects are ignored in a first approximation. The quoted temperature values have an estimated experimental uncertainty of ±0.1 K. The geometry of the experiment is shown in Figure 1a. Microscopic images are collected on video and digitized using a frame grabber. In all cases, the structure factor $S(\mathbf{q},\dot{\gamma})$ calculated numerically from the fast Fourier transform (FFT) of the digitized real-space image [the "power spectrum" $\langle\psi_{\mathbf{q}}\psi_{-\mathbf{q}}\rangle$] closely resembles the measured light-scattering pattern, as shown in Figure 1.

IV. Results and Discussion

A. Droplet Deformation and Breakup. Figure 3 shows light-scattering/micrograph pairs for a low-molecular-weight PS/PB blend undergoing spinodal decomposition in the presence of steady shear flow. Stabilized in the weak-shear limit, initially spherical droplets elongate into ellipsoids and then break repeatedly with increasing $\dot{\gamma}$, eventually giving way to extended domains that scatter light with extreme anisotropy. In the strong-shear limit, elongated domains coalesce into a stringlike pattern. The projection of the scattering intensity perpendicular ($\hat{\mathbf{z}}$) and parallel ($\hat{\mathbf{x}}$) to the flow direction is shown in Figure 4, and suggests asymptotic Porod behavior[34] persisting normal to the flow direction at intermediate shear rates. When the string width becomes comparable to the thermal correlation length, the mixture becomes homogeneous.[17]

We can fit projections of the scattering intensity along the $\hat{\mathbf{x}}$ and $\hat{\mathbf{z}}$ directions to the squared-Lorentzian expression

$$S(q_{x,z},\dot{\gamma}) = \frac{S_{x,z}(0,\dot{\gamma})}{\{1 + [\tilde{R}_{x,z}(\dot{\gamma})q_{x,z}]^2\}^2} \qquad (3)$$

Such an equation is often used to interpolate the Guinier (low-q) and Porod (high-q) limits for scattering from random, isotropic structures with sharp interfaces.[34] We heuristically extend it to the anisotropic structures of interest here by considering independent projections perpendicular and parallel to the flow direction. Anisotropy in the $q = 0$ scattering is unphysical,

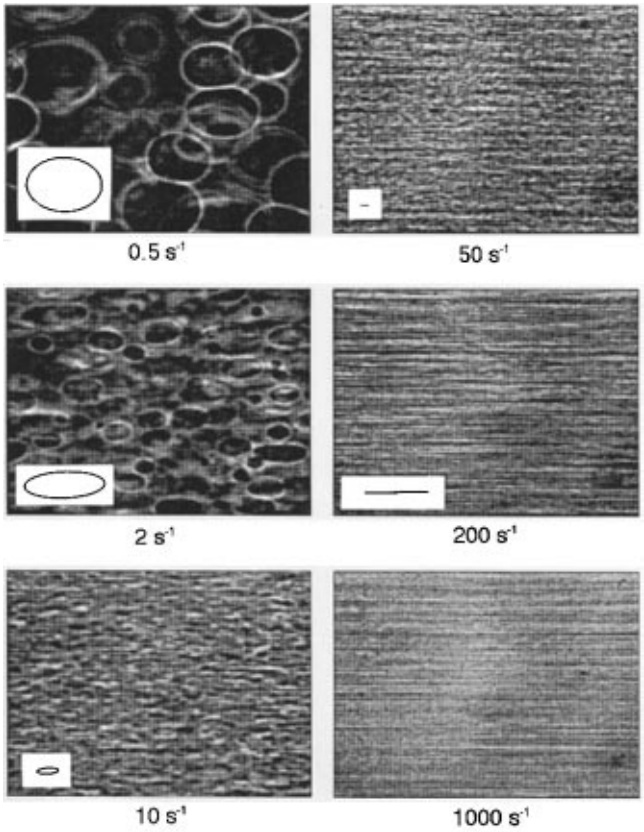

Figure 6. Digital video micrographs of a coexisting critical mixture [30/70 PS/PB ($96.4 \times 10^3/22 \times 10^3$), 8% polymer in dioctylphthalate (DOP) at 60 °C, $T_c(0) - T = 8$ K] under simple shear flow. The geometry and scale are as specified in Figure 1. The elliptical shapes (insets) are cross sections of the deformed droplets within the theoretical framework described in the text. Each time a droplet ruptures, the composition difference between droplet and matrix decreases, pushing the mixture toward the stability limit and thus decreasing the droplet surface tension. As a consequence, the domains can be stretched further before bursting. The bare stress−relaxation time is $\tau_{c0} = 0.29$ s.

but these can be viewed as effective quantities over the q range in question. Although the fits are reasonable, the physical significance of $\tilde{R}_x(\dot{\gamma})$ and $\tilde{R}_z(\dot{\gamma})$ is unclear. For the average droplet sizes in question, the probed q range is typically well above the Guinier limit, and the scattering is dominated by the interfacial contribution. Figure 5 shows $\tilde{R}_x(\dot{\gamma})$ and $\tilde{R}_z(\dot{\gamma})$ for the data in Figure 4. As can be seen by comparison with the micrographs (Figure 3), the values are comparable to the smallest end of the droplet size distribution and suggest an overall decrease with increasing shear rate. In the breakup region, ($1\ s^{-1} < \dot{\gamma} < 20\ s^{-1}$), $\tilde{R}_z(\dot{\gamma})$ appears to become slightly enhanced.

A quantitative description of the crossover from droplets to strings must address droplet breakup. As a first approximation, we consider a single droplet of average size and assume that it breaks into two identical fragments.[17] From conservation of volume, the droplet size, stress−relaxation time, and threshold shear rate after n breaking transitions are given by the recursion relations

$$R(n) = 2^{-n/3} R_0 \qquad \tau_c(n) = 2^{-n/3}\tau_c \qquad \dot{\gamma}_c(n) = 2^{n/3}\dot{\gamma}_c$$

respectively, and the aspect ratio ζ is given by eq 1 with $x = \tau_c(n)\dot{\gamma}$. To account for the softening of the interfacial tension with shear, we use eq 2 to get

$$\tau_c(n) = 2^{-n/3}\tau_{c0}(1 - A\tilde{\gamma}^a)^{-2\nu} \tag{4}$$

where $\tilde{\gamma} = \tau_{c0}\dot{\gamma}$ is the reduced shear rate and $a = 1/3\nu$. At a given temperature, the only adjustable parameter is the bare stress−relaxation time τ_{c0}, which is determined from a fit of the average ζ vs $\dot{\gamma}$ in the weak-shear limit before the droplets, on average, start to break.[17]

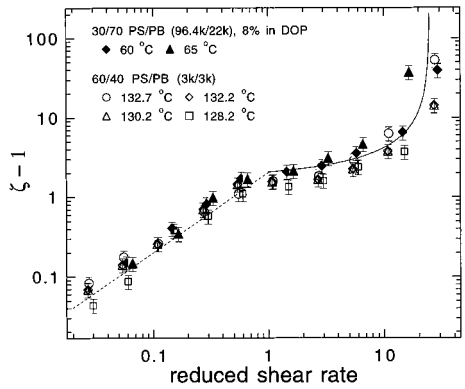

Figure 7. Log−log plot of the dimensionless deviation from isotropic droplets as a function of reduced shear rate, or Deborah number, for a variety of polymer mixtures in the vicinity of a critical point. The dashed line represents the weak-shear (Taylor) limit, while the solid line is the crossover to strong-shear as described in the text. There are no adjustable parameters. The onset of nonclassical behavior corresponds to $\tilde{\gamma} \sim 1$, which is when the droplets, on average, start to break. The corresponding τ_{c0} values are; 0.29 (closed diamonds), 0.33 (closed triangles), 0.55 (open circles), 0.54 (open diamonds), 0.5 (open triangles), and 0.3 s (open squares).

This description is leading order in the sense that it neglects shear thinning, ignores the viscosity difference between droplet and matrix, assumes mean-field breaking transitions, ignores droplet interactions, and greatly oversimplifies the breakup of an isolated droplet. A comparison of the data for a critical PS/PB/DOP mixture with the above model is shown in Figure 6. The elliptical domain shapes (insets) were generated in the following way. At low $\dot{\gamma}$ before breakup, a fit of the average aspect ratio (rescaled assuming $\theta \approx \pi/9$ in the vicinity of the breakup) as a function of $\dot{\gamma}$ gives τ_{c0}. By using the initial estimate $\dot{\gamma}_{c0} \sim 1/2\tau_{c0} \sim 1.5\ s^{-1}$, applying the recursion relations at each consecutive breaking transition, and using eq 4 to account for the softening of the interfacial tension,[35] we generate the average ζ as a function of $\dot{\gamma}$. The average droplet dimensions are then given by

$$R_\perp(\dot{\gamma}) = \zeta^{-1/3} R_n$$

$$R_\parallel(\dot{\gamma}) = \zeta^{2/3} R_n \tag{5}$$

where $R_n = 2^{-n/3}R_0$ and n is the number of breaking transitions that have occurred, on average, up to the shear rate of interest. The aspect ratios and relative sizes can be compared directly with the micrographs. Stringlike behavior emerges at around 100−200 s^{-1}. Beyond this shear rate, the model is inapplicable. The model gives a good *semiquantitative* description of the evolution from droplets to strings for diluted high-molecular-weight and pure low-molecular-weight PS/PB blends near the critical point.

Weak-to-intermediate shear data for a variety of temperatures and shear rates should collapse onto a universal scaling curve when expressed in terms of $\tilde{\gamma}$.

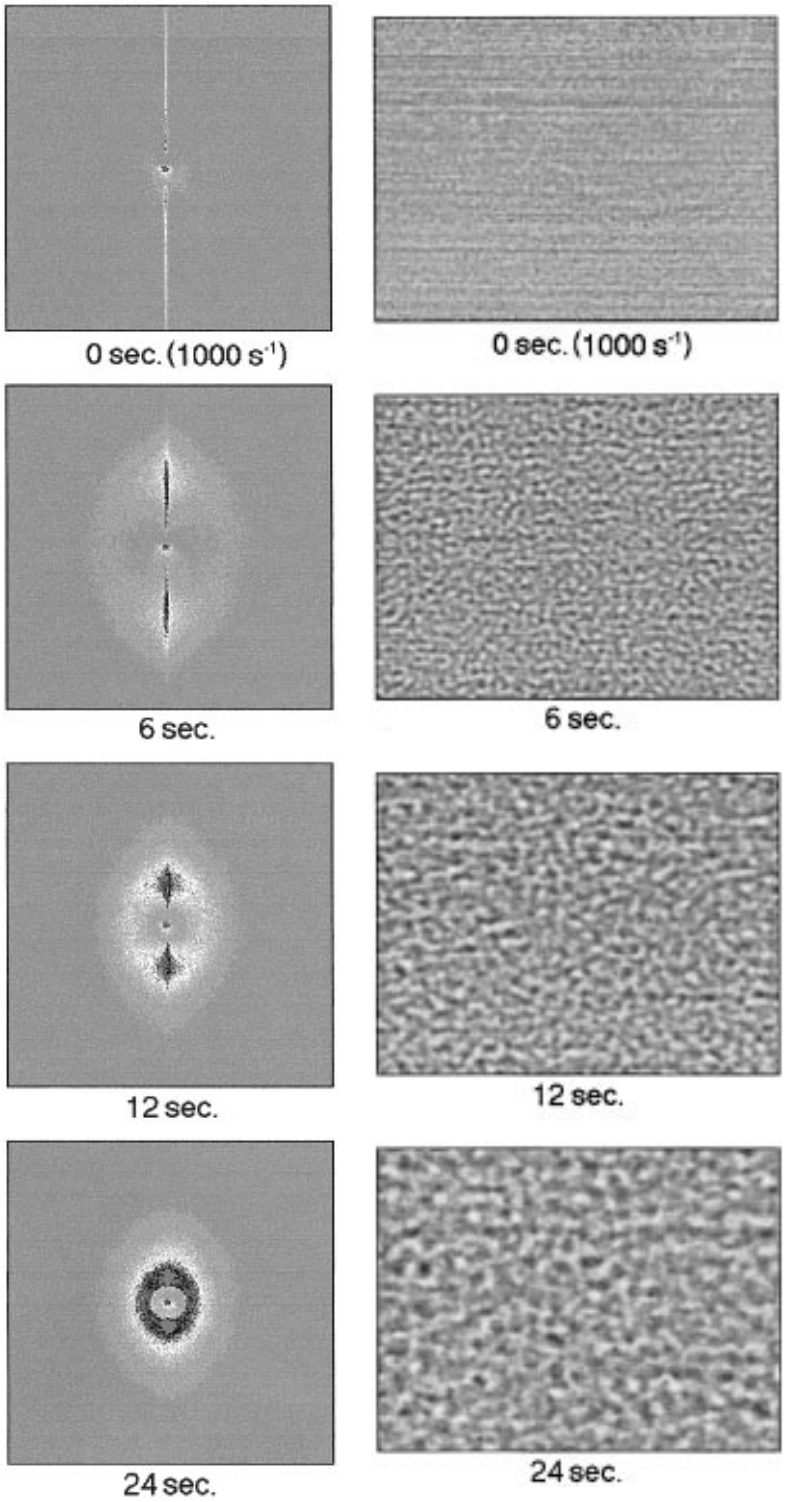

Figure 8. Spinodal decomposition and stress relaxation in an unstable PS/PB mixture (50/50 96.4 × 10^3/22 × 10^3, 8% polymer in DOP, T = 55 °C, T_s = 60 °C) after cessation of shear. The times after shear quenching are shown in seconds. The mixture exhibits a string pattern at a shear rate of 1000 s^{-1}. After the flow is terminated, a spinodal ring is superimposed on an anisotropic scattering pattern.

This is shown in Figure 7 for both pure low-molecular-weight and diluted high-molecular-weight PS/PB blends at different temperatures and shear rates in the vicinity of ϕ_c. The dashed line is the weak-shear result $\zeta - 1 = 2\tilde{\gamma}$ that follows from eq 1, and the solid line is the crossover behavior calculated from eq 1 using the aspect ratio halfway between each breaking transition. The two limits are separated by $\tilde{\gamma} \sim 1$, which is where the droplets start to break. String patterns emerge at lower shear rates as one moves closer to the quiescent critical temperature $T_c(0)$. It is important to note that in contrast to the one-phase case, the bare relaxation time is not a true equilibrium quantity but is characteristic of a coarsening instability that has been stabilized by the flow.

B. Spinodal Decomposition and Stress Relaxation. The mixing effect of the flow is central to the above interpretation, as this is what leads to the softening of the interfacial tension. More direct probes of domain composition under shear are thus desirable.

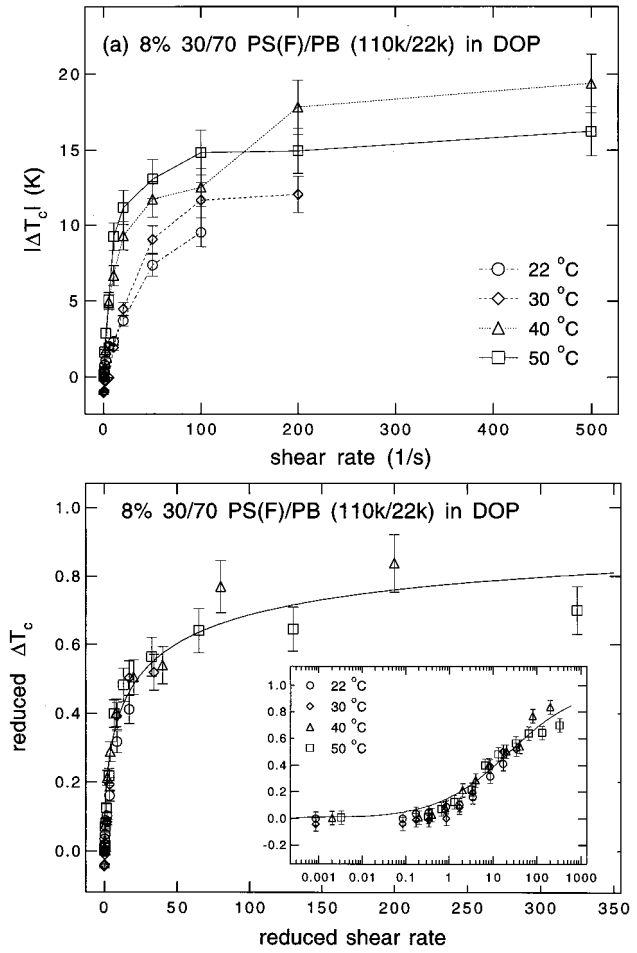

Figure 9. (a) Shear-induced shift in T_c for a diluted 30/70 PS(F)/PB blend [$110 \times 10^3/22 \times 10^3$, 8% polymer in DOP, $T_c(0) = 86.5$ °C] where the PS has been labeled with a fluorophore. In b, the T_c shift has been reduced by its "saturated" value and $\dot{\gamma}$ has been rescaled by τ_{c0}. The inset is a linear log plot of the data over 6 decades in reduced shear rate, and the line is the fit to eq 6. Mixing begins when the shear rate becomes comparable to $1/\tau_{c0}$ or for $\tilde{\gamma} \sim 1$, which is when the droplets start to break (Figure 7). The corresponding τ_{c0} values are 0.17 (open circles), 0.17 (open diamonds), 0.4 (open triangles), and 0.65 s (open squares).

Evidence for thermodynamic mixing or "homogenization" associated with the formation of string patterns can be found from the type of cessation-of-shear experiment[36] shown in Figure 8. After the system has reached a steady-state stringlike pattern, the flow is terminated and the time evolution of the structure studied with light scattering and microscopy. In addition to the droplet stress−relaxation and coalescence that are apparent in the micrographs, the light-scattering patterns reveal a faint spinodal ring at high q that slowly merges with the low-q structure. Such behavior is consistent with shear-induced mixing in the two-phase region.

The fact that only one spinodal ring is apparent in the data suggests that the rate at which the matrix decomposes into the equilibrium composition profile is comparable to the analogous rate inside the droplets. Also of interest is the relatively long time (on the order of 20 s) required for the anisotropy in the domain structure to relax. Although this is consistent with a significantly reduced surface tension in the string state relative to that in the stabilized low-shear state, noncritical stringlike filaments having a high surface tension are also observed to breakup gradually into isotropic droplets upon the cessation of flow.[21] Detailed shear-quench experiments have been carried out, and the results will be presented elsewhere.

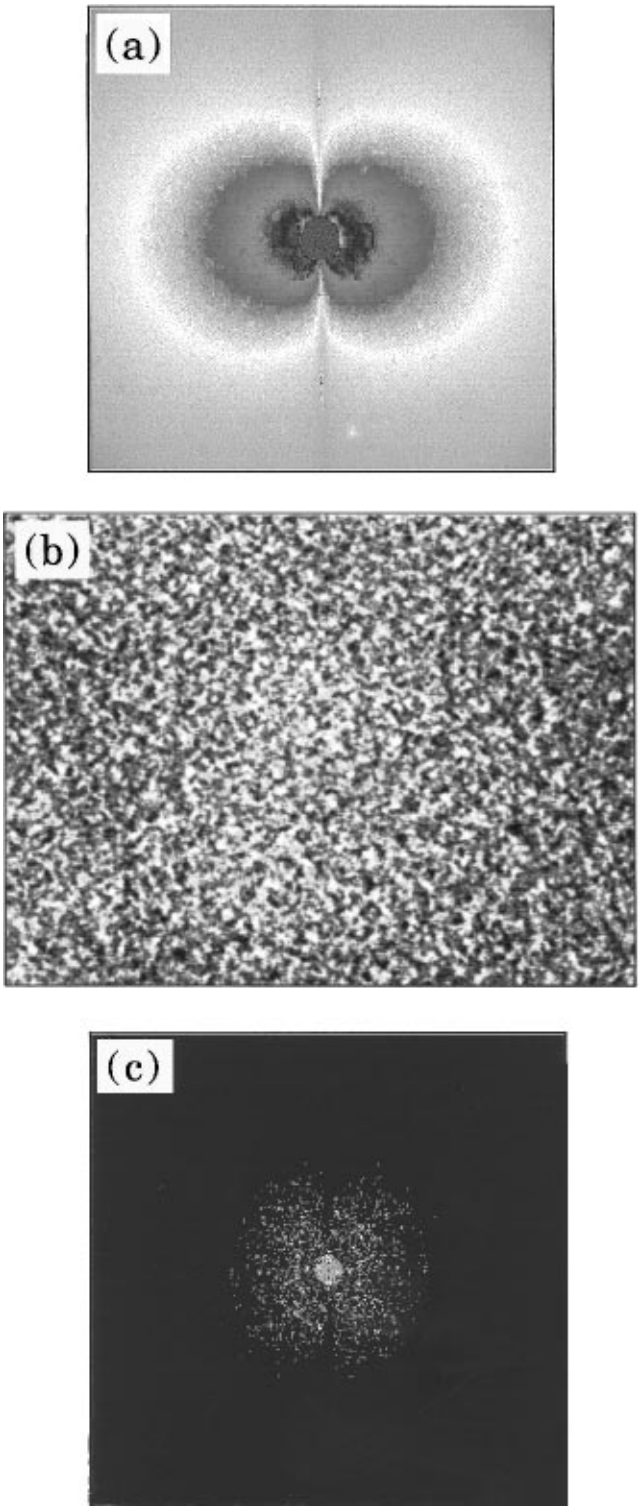

Figure 10. Light-scattering/micrograph pair for a phase-separated blend of high-molecular-weight PS(F)/PB [50/50 $110 \times 10^3/22 \times 10^3$, 8% polymer in DOP, $T = 22$ °C, $T_s(0) = 77$ °C] showing a well-defined butterfly pattern at a shear rate of 1000 s^{-1}. The top figure (a) is the light-scattering pattern, the middle figure (b) is the micrograph, and the lower figure (c) is the structure factor calculated numerically from the FFT of the digitized image. The geometry is as specified in Figure 1.

C. Shear-Induced Homogenization. In the diluted high-molecular-weight PS/PB/DOP blends, label-

ing the polystyrene with the fluorescent dye NBD chloride allows a direct measurement of domain composition under shear using fluorescence microscopy, which in turn allows us to determine $T_c(\dot{\gamma})$ in the two-phase region. The details of the experimental technique are described elsewhere.[18] Because of the tendency for the dye to quench at high temperatures, however, such measurements are presently restricted to temperatures well below $T_c(0)$ where the components are strongly incompatible. As shown in Figure 9a, $\Delta T_c(\dot{\gamma}) = T_c(0) - T_c(\dot{\gamma})$ determined in this way shows a tendency to saturate at extremely high shear rates. Simultaneous phase-contrast micrographs can be used to determine τ_{c0} as in the previous section. When the shear rate is rescaled by τ_{co} and $\Delta T_c(\dot{\gamma})$ is reduced by its saturated ($\dot{\gamma} \rightarrow \infty$) value, the data collapse onto the universal scaling curve shown in Figure 9b. The line is the empirical expression

$$\frac{\Delta T_c(\tilde{\gamma})}{\Delta T_{c\infty}} = \frac{0.2\tilde{\gamma}^{0.44}}{1 + 0.2\tilde{\gamma}^{0.44}} \qquad (6)$$

where $\tilde{\gamma} = \tau_{c0}\dot{\gamma}$ and $\Delta T_{c\infty} \approx 24$ K is the saturated T_c shift.[18] At weak shear, eq 6 reduces to a simple power law that is compatible with the leading-order MCRG theory, but at very high $\dot{\gamma}$, such a description breaks down.

A clue into the origin of such a "mixing plateau" might lie in the observation that the shear rates where it occurs tend to coincide with the emergence of the type of "butterfly" pattern shown in Figure 10. This ubiquitous shape appears in solutions of semidilute entangled polymers under shear,[14,37] wormlike micelles under shear,[38] swollen gels and networks under uniaxial strain,[39] electrorheological fluids in an external electric field,[40] and aligned nematic polymer liquid crystals.[41] Although not obviously universal in nature, its presence in entangled polymer solutions has been linked to viscoelasticity and shear-induced *unmixing*.[23−25,42,43] This latter observation is particularly interesting in light of the fact that it appears here in connection with a *threshold* to shear-induced mixing in diluted high-molecular-weight blends. The pure low-molecular-weight PS/PB blends used in this study did not exhibit this pattern. Its appearance in diluted *blends* is not presently well understood but may also be linked to viscoelastic effects.[44] Experiments are underway that may shed more light on this behavior.

V. Outlook and Conclusions

From the domain morphology as a function of temperature and shear rate, we can construct a "morphology diagram" as depicted in Figure 11 for a diluted high-molecular-weight PS/PB blend. Analogous stringlike behavior is found for critical blends of PB and polyisoprene (PI),[45] which, in contrast to the PS/PB system, exhibit phase separation upon heating. For temperatures in modest proximity to $T_c(0)$, the MCRG theory, when combined with the Taylor model of droplet breakup, offers a remarkably accurate and physically simple picture of the shear response of polymer blends. This has been demonstrated to be the case in a broad class of critical fluids, which speaks to the concept of universality in dynamic critical phenomena. The apparent inadequacy of the leading-order MCRG description at high shear rates well into the equilibrium two-phase region of polymeric mixtures is not surprising, as in its original form it represents an asymptotic calculation

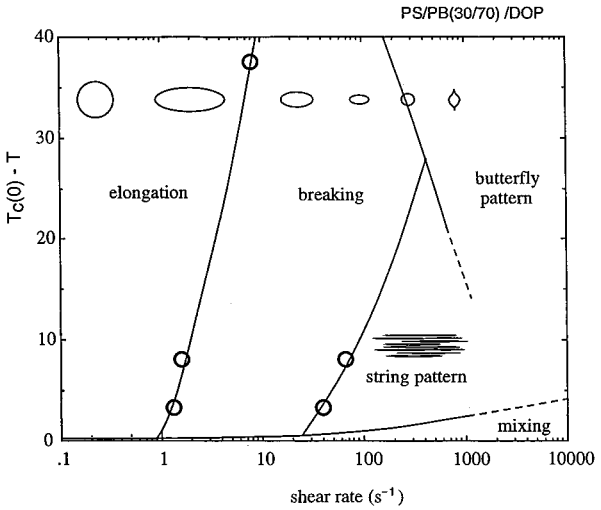

Figure 11. Morphology diagram for a 30/70 PS/PB (8% 96.4 × 10^3/22 × 10^3 in DOP) critical mixture. The vertical axis is the deviation between the sample temperature and the equilibrium critical temperature of 68 °C. The data markers (open circles) are measured transition points. Close to $T_c(0)$, elongation gives way to fragmentation, which gives way to strings and eventually homogenization. For the deeper quenches where butterfly patterns emerge, the strong-shear response is not well-understood.

close to $T_c(0)$ for Newtonian components that assumes some sense of proximity to an equilibrium state.

Scaling in terms of reduced variables appears to remain intact in the plateau region where the fluid is strongly driven. The reason for this might lie in the fact that the low-shear stress−relaxation times used to reduce $\dot{\gamma}$ are not true equilibrium quantities but are characteristic of a coarsening thermodynamic instability that has been stabilized by the flow, and thus a degree of the nonequilibrium nature of the fluid has already been taken into account. The fact that the shear response changes radically when $\dot{\gamma}$ becomes comparable to a characteristic stress−relaxation rate is indeed intuitive. Particularly appealing is the observation that mixing or *homogenization* commences when the droplets first start to break, as a simple way for the composition profile to evolve is for the domain interface to rupture.

Acknowledgment. We acknowledge fruitful and useful discussions with E. Amis, A. Nakatani, J. Douglas, B. Lee, and H. Jeon.

References and Notes

(1) de Gennes, P. G. *Scaling Concepts in Polymer Physics*; Cornell University: Ithaca, NY, 1979.
(2) See, for example: Sakellarides, S. L.; McHugh, A. J. *Polym. Eng. Sci.* **1987**, *27*, 1662 and references therein.
(3) (a) Onuki, A.; Kawasaki, K. *Ann. Phys.* **1979**, *121*, 456. (b) Onuki, A.; Kawasaki, K. *Prog. Theor. Phys. Suppl.* **1978**, *64*, 436. (c) Onuki, A.; Yamazaki, K.; Kawasaki, K. *Ann. Phys.* **1981**, *131*, 217. (d) Onuki, A. *Phys. A* **1986**, *140*, 204.
(4) (a) Onuki, A. *Phys. Rev. A* **1986**, *34*, R3528. (b) *Phys. A* **1986**, *140*, 204. (c) *Int. J. Thermophys.* **1989**, *10*, 293.
(5) Onuki, A. *Phys. Rev. A* **1987**, *35*, 5149.
(6) (a) Bates, F. S.; Rosedale, J. H.; Stepanek, P.; Lodge, T. P.; Wiltzius, P.; Fredrickson, G. H.; Hjelm, R. P. *Phys. Rev. Lett.* **1990**, *65*, 1893. (b) Stepanek, P.; Lodge, T. P.; Kedrowski, C.; Bates, F. S. *J. Chem. Phys.* **1991**, *94*, 8289.
(7) (a) Schwahn, D.; Mortensen, K.; Yee-Madeira, H. *Phys. Rev. Lett.* **1987**, *15*, 1544. (b) Janssen, S.; Schwahn, D.; Springer, T. *Phys. Rev. Lett.* **1992**, *68*, 3180.
(8) Meier, G.; Momper, B.; Fischer, E. W. *J. Chem. Phys.* **1992**, *97*, 5884.
(9) Miyashita, N.; Nose, T. *J. Chem. Phys.* **1994**, *100*, 6028.

(10) (a) Hair, D. W.; Hobbie, E. K.; Nakatani, A. I.; Han, C. C. *J. Chem. Phys.* **1992**, *96*, 9133. (b) Hobbie, E. K.; Reed, L.; Huang, C. C.; Han, C. C. *Phys. Rev. E* **1993**, *48*, 1579.
(11) (a) Beysens, D.; Gbadamassi, M.; Boyer, L. *Phys. Rev. Lett.* **1979**, *43*, 1253. (b) Beysens, D.; Gbadamassi, M. *J. Phys. (Paris)* **1979**, *40*, L565. (c) Beysens, D.; Gbadamassi, M. *Phys. Rev. A* **1980**, *22*, 2250. (d) Beysens, D.; Gbadamassi, M.; Moncef-Bouanz, B. *Phys. Rev. A* **1983**, *28*, 2491.
(12) (a) Hobbie, E. K.; Nakatani, A. I.; Han, C. C. *Mod. Phys. Lett. B* **1994**, *8*, 1143 and references therein. (b) Hobbie, E. K.; Hair, D. W.; Nakatani, A. I.; Han, C. C. *Phys. Rev. Lett.* **1992**, *69*, 1951. (c) Nakatani, A.; Kim, H.; Takahashi, Y.; Matsushita, Y.; Takano, A.; Bauer, B.; Han, C. *J. Chem Phys.* **1990**, *93*, 795.
(13) Hobbie, E. K.; Nakatani, A. I.; Yajima, H.; Douglas, J. F.; Han, C. C. *Phys. Rev. E* **1996**, *53*, R4322.
(14) Hashimoto, T.; Matsuzaka, K.; Moses, E.; Onuki, A. *Phys. Rev. Lett.* **1995**, *74*, 126.
(15) Kim, S.; Yu, J. W.; Han, C. C. *Rev. Sci. Instrum.* **1996**, *67*, 3940.
(16) Moses, E.; Kume, T.; Hashimoto, T. *Phys. Rev. Lett.* **1994**, *72*, 2037.
(17) Hobbie, E. K.; Kim, S.; Han, C. C. *Phys. Rev. E* **1996**, *54*, R5909.
(18) Yu, J. W.; Douglas, J. F.; Hobbie, E. K.; Kim, S.; Han, C. C. *Phys. Rev. Lett.* **1997**, *78*, 2664.
(19) (a) Taylor, G. I. *Proc. R. Soc. London* **1932**, *A138*, 41. (b) *Proc. R. Soc. London* **1934**, *A146*, 501.
(20) (a) Rallison, J. M.; *J. Fluid Mech.* **1981**, *209*, 465. (b) *Annu. Rev. Fluid Mech.* **1984**, *16*, 45. (c) Torza, S.; Cox, R. G.; Mason, S. G. *J. Colloid Interface Sci.* **1972**, *38*, 395. (d) Rumscheidt, F. D.; Mason, S. G. *J. Colloid Sci.* **1961**, *16*, 238.
(21) Tomotika, S. *Proc. R. Soc. London* **1932**, *A150*, 322.
(22) Fredrickson, G. H.; Bates, F. S. *J. Chem. Phys.* **1986**, *85*, 633.
(23) Helfand, E.; Fredrickson, G. H. *Phys. Rev. Lett.* **1989**, *62*, 2468.
(24) Onuki, A. *Phys. Rev. Lett.* **1989**, *62*, 2472.
(25) Milner, S. T. *Phys. Rev. Lett.* **1991**, *66*, 1477.
(26) Hohenberg, P. C.; Halperin, B. I. *Rev. Mod. Phys.* **1977**, *49*, 435.
(27) Douglas, J. F. *Macromolecules* **1992**, *25*, 1468. See also ref 12.
(28) (a) Hair, D. E. W.; Hobbie, E. K.; Douglas, J. F.; Han, C. C. *Phys. Rev. Lett.* **1992**, *20*, 2476. (b) Yajima, H.; Hair, D. W.; Nakatani, A. I.; Douglas, J. F.; Han, C. C. *Phys. Rev. B* **1993**, *47*, 12 268.
(29) For high-molecular-weight blends, a true shift in T_c is not expected. Evidence for this can be found in the shear response as measured with SANS, which shows no change in scattering intensity perpendicular to the flow direction. See refs 12, 13, and 27.
(30) (a) Goldburg, W. I.; Min, K. Y. *Phys. A* **1994**, *A204*, 246. (b) Hashimoto, T.; Takebe, T.; Fujioka, K. In *Dynamics and Patterns in Complex Fluids*; Onuki, A., Kawasaki, K., Eds.; Springer: Berlin, 1990; p 86.
(31) The weak and strong shear limits are defined by $\tau_c\dot{\gamma} < 1$ and $\tau_c\dot{\gamma} > 1$, respectively. For a phase-separated critical mixture, there will be a relaxation time associated with thermal (zero-mean) fluctuations around an average, as in the one-phase region. There is also a characteristic relaxation time associated with the coarsening droplets themselves. Fluorescence microscopy studies of shear-induced mixing suggest that it is the latter that should be used in the reduced-variable description.
(32) For a noncritical fluid with small $\Delta\eta$, the aspect ratio never exceeds the breakup value $\zeta_{max} \sim 2-3$.
(33) Moldover, M. R. *Phys. Rev. A* **1985**, *31*, 1022.
(34) For a two-phase system with sharp interfaces, the radial-distribution function $g(r)$ decreases linearly with r at small r, implying that $S(q)$ scales as q^{-4} at high q [Porod, G. *Kolloid Z.* **1951**, *124*, 82]. Scattering from a random collection of randomly-shaped, isotropic structures with sharp interfaces has been discussed by Debye [Debye, P.; Anderson, H. R.; Brumberger, H. *J. Appl. Phys.* **1957**, *28*, 679].
(35) The scatter in the data is such that we do not attempt to resolve exact values of ν and A. Strictly speaking, the apparent critical exponents and amplitudes may be subject to a "Fisher Renormalization" upon dilution of a pure blend so that these quantities are not completely system independent. In eq 4, we use the approximate values $2\nu \approx 1$, $1/3\nu \approx {}^1/_2$, and $A \approx {}^1/_{10}$.
(36) Takebe, T.; Sawaoka, R.; Hashimoto, T. *J. Chem. Phys.* **1989**, *91*, 4369.
(37) (a) Kume, T.; Hashimoto, T. In *Flow-Induced Structures in Polymers*; ACS Symposium Series No. 597; Nakatani, A. I., Dadmun, M. D., Eds.; American Chemical Society: Washington, DC, 1994; p 35. (b) Kim, S.; *et al.* Unpublished results.
(38) (a) Kadoma, I.; van Egmond, J. *Phys. Rev. Lett.* **1996**, *76*, 4432. (b) Slawecki, T.; *et al.* Unpublished results.
(39) (a) Mendes, E.; Oeser, R.; Hayes, C.; Boue, F.; Bastide, J. *Macromolecules* **1996**, *29*, 5574. (b) Geissler, E.; Horkay, F.; Hecht, A. *J. Chem. Phys.* **1995**, *102*, 9129. (c) Bastide, J.; Leibler, L.; Prost, J. *Macromolecules* **1990**, *23*, 1821. (c) Mours, M.; Winter, H. *Macromolecules* **1996**, *29*, 7221. (d) Panyukov, S.; Rabin, Y. *Macromolecules* **1996**, *29*, 7960.
(40) (a) Halsey, T. C. *Science* **1992**, *258*, 761. (b) Kamien, R.; Le Doussal, P.; Nelson, D. R. *Phys. Rev. A* **1992**, *45*, 8727.
(41) Ao, X.; Wen, X.; Meyer, R. B. *Phys. A* **1991**, *A176*, 63.
(42) (a) Ver Strate, G.; Philippoff, W. *Polym. Lett.* **1974**, *12*, 276. (b) Rangel-Nafaile, C.; Metzner, A.; Wissbrun, K. *Macromolecules* **1984**, *17*, 1187. (c) Wu, X.; Pine, D.; Dixon, P. *Phys. Rev. Lett.* **1991**, *66*, 2408. (d) Dixon, P.; Pine, D.; Wu, X. *Phys. Rev. Lett.* **1992**, *68*, 2239.
(43) Milner, S. T. *Phys. Rev. E* **1993**, *48*, 3874.
(44) Onuki, A.; Taniguchi, T. *J. Chem. Phys.* **1997**, *106*, 5761.
(45) Jeon, H.; *et al.* Unpublished results.

MA9707648